ISSN 1061-8309, Russian Journal of Nondestructive Testing, 2015, Vol. 51, No. 5, pp. 308–314. © Pleiades Publishing, Ltd., 2015.
Original Russian Text © D.Ya. Sukhanov, E.S. Sovpel', 2015, published in Defektoskopiya, 2015, Vol. 51, No. 5, pp. 58–64.

MAGNETIC AND ELECTRICAL METHODS

A Magnetic-Induction Introscope for Flaw Detection of Metal Objects

D. Ya. Sukhanov and E. S. Sovpel'

Tomsk National Research State University, Tomsk, Russia

e-mail: sdy@mail.tsu.ru; berzinaelena@mail.ru

Received September 23, 2014

Abstract—An apparatus for obtaining two-dimensional images of sheet-metal products that is based on a scanning matrix of spiral induction coils has been designed. It was experimentally shown that it is possible to detect flaws and objects that are hidden behind metallic barriers. The scanning area was 37 × 32 cm and the measurement step was 5 mm. Special treatment allows one to restore the distribution of induction currents in conductive objects from the remote measurement of the normal-component distribution of the magnetic induction vector on a plane.

Keywords: magnetic induction introscopy, induction current, two-dimensional visualization

DOI: 10.1134/S1061830915050095

INTRODUCTION

Flaw detection using magnetic-induction methods has wide application in modern industry, medicine, and geology. The magnetic-induction methods allow one to carry out the introscopy of electroconductive media and detection of metals.

There are approaches to solving inverse problems of magnetostatics [1] for the restoration of object images with magnetic-permeability contrasts that are based on measuring disturbances of a constant magnetic field. However, to study nonmagnetic electroconductive materials, it is expedient to consider application of alternating magnetic fields that induce currents in the studied objects [2]. The restoration of the induction current distribution will assist one in determining the shapes of objects and the existence of defects.

Studies of different alternating magnetic sensors [3, 4] have shown that it is expedient to use magnetic-induction coils instead of Hall-effect devices or other solid-state sensors. In magnetic-induction tomography measurement schemes with different positions of coil-sources and receiving coils are used. For example, transmission multiposition schemes [5] that are used in medical diagnostics [6, 7] have been developed. With one-sided access to a studied object it is expedient to use differential magnetic-induction sensors [8, 9]. However, it is technically complicated to manufacture matrices of similar sensors.

The inverse problems of magnetic-induction tomography are incorrect problems with weak stability, since magnetic fields are weakly localized, rapidly decrease with distance, and, as a rule, have a narrow spatial spectrum. Due to this fact, low noise in the measurements leads to substantial errors when tomograms are restored [10], which requires regularization [11].

In this work we present a device (based on a matrix of planar rectangular spectral coils) for restoring the images of electroconductive objects from magnetic-induction measurements, when the access to the object is one-sided. It is shown that it is possible to restore the induction-current distribution from the measurement results. This device can be used in problems of the flaw detection of planar electroconductive objects.

THE MEASUREMENT SCHEME

Let us consider the measurement scheme that is shown in Fig. 1. We used a rectangular coil as a low alternating magnetic-field source. The coil field induces induction currents in an electroconductive object, which generate a secondary magnetic field. Using the induction-coil matrix we will measure the z-component of the vector of the magnetic induction in a flat rectangular region at some distance, h, from the object in the plane that is parallel to the coil–source plane. First, we will measure the background field

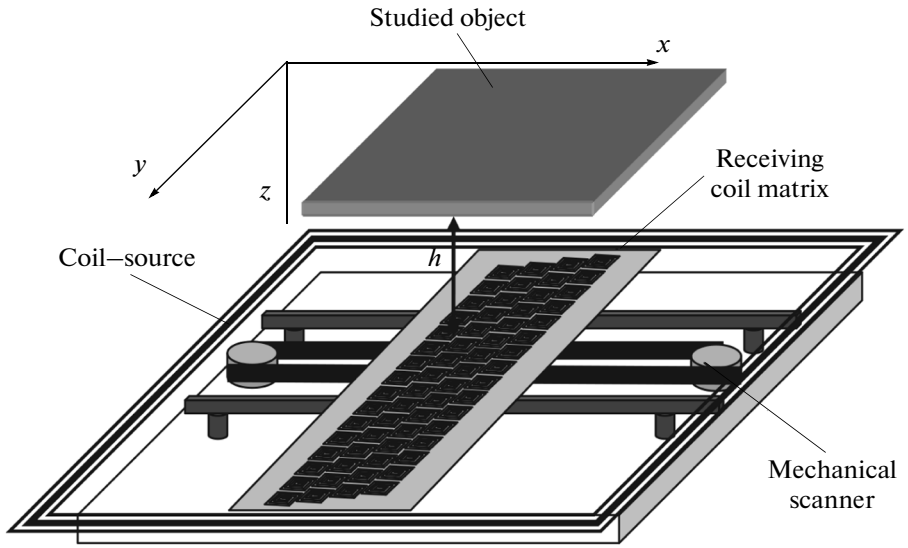

Fig. 1. The measurement scheme.

without the object, i.e., the coil–source field; then (measuring with the object), the field of the source is subtracted; thus, only the field that is caused by induction currents in the object remains.

We assume that the object is flat, i.e., the currents that were induced in it have only X- and Y-components and the approximations of quasimagnetostatics are also correct. We consider that the field source is the induction currents of the studied object, since the field of the coil–source is removed by subtracting the background. In [12] the numerical simulation of this system was performed and a method for the restoration of the induction-current distribution was proposed.

RESTORATION OF THE INDUCTION-CURRENT DISTRIBUTION

According to [12], the vector potential is restored from the current-density distribution using the solution in delayed potentials, which can be written in the spatial spectrum area as:

$$\tilde{A}(k_x, k_y, h) = \tilde{j}(k_x, k_y)\tilde{H}(k_x, k_y), \tag{1}$$

where $\tilde{j}(k_x, k_y) = \int_{-\infty}^{\infty}\int_{-\infty}^{\infty} j(x, y, 0)e^{ik_x x + ik_y y}(dx)dy$, $\tilde{H}(k_x,k_y) = \mu\mu_0 \dfrac{\exp(-h\sqrt{k_x^2 + k_y^2})}{8\pi^2\sqrt{k_x^2 + k_y^2}}$.

The current-density distribution can then be carried out using the inverse convolution operation:

$$\tilde{j}(k_x, k_y) = \frac{\tilde{A}(k_x, k_y, h)}{\tilde{H}(k_x, k_y)}. \tag{2}$$

However, it is assumed that only the z-component of the magnetic-induction vector in the plane $\mathbf{z} = h$ is measured, i.e., $B_z(x, y, z = h)$. It is necessary to calculate the currents j_x and j_y from the value B_z. First, let us express the vector A via the magnetic-induction vector; in this case, let us take into account that $A_z = 0$

$$B = \mathrm{rot}A, \text{ or } \begin{pmatrix} B_x \\ B_y \\ B_z \end{pmatrix} = \begin{pmatrix} -\dfrac{\partial A_y}{\partial z} \\ \dfrac{\partial A_x}{\partial z} \\ \dfrac{\partial A_y}{\partial x} - \dfrac{\partial A_x}{\partial y} \end{pmatrix}.$$

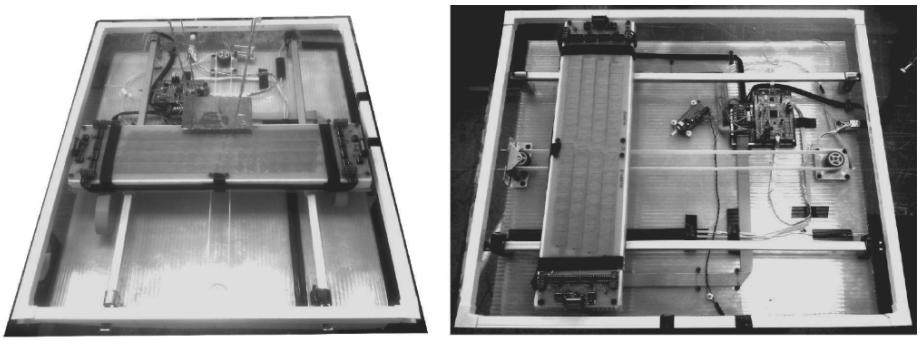

Fig. 2. Photographs of the experimental setup.

We only know the component B_z and for it one can write the equation $B_z = \frac{\partial A_y}{\partial x} - \frac{\partial A_x}{\partial y}$, which can be written in the spatial frequency region as:

$$\tilde{B}_z = ik_x\tilde{A}_y - ik_y\tilde{A}_x. \quad (3)$$

By dividing expression (3) by $\tilde{H}(k_x, k_y)$ and taking expression (2) into account we obtain

$$\frac{\tilde{B}_z}{\tilde{H}} = ik_x\tilde{j}_y - ik_y\tilde{j}_x. \quad (4)$$

It is impossible to calculate the two values $\tilde{j}_x$ and $\tilde{j}_y$ from expression (4); one more equation is required. We assume that the currents in the object are eddy currents, i.e., they satisfy the equation div$j = 0$, and since $j_z = 0$, then $\frac{\partial j_x}{\partial x} = \left(-\frac{\partial j_y}{\partial y}\right)$, or in the spatial frequency spectrum $ik_x\tilde{j}_x = -ik_y\tilde{j}_y$, or $\tilde{j}_y = -\frac{k_x}{k_y}\tilde{j}_x$. Reasoning from these equations, it is possible to express the spatial spectra of the components of the current-density vector and, further, to restore the induction current distribution via the inverse Fourier transformation:

$$j_x(x,y) = \frac{1}{4\pi^2}\int_{-\infty}^{\infty}\int_{-\infty}^{\infty}\frac{ik_y\tilde{B}_z(k_x, k_y)}{\tilde{H}(k_x, k_y)(k_x^2 + k_y^2)}e^{-ik_xx - ik_yy}dk_x(dk_y), \quad (5)$$

$$j_y(x,y) = \frac{1}{4\pi^2}\int_{-\infty}^{\infty}\int_{-\infty}^{\infty}\frac{-ik_x\tilde{B}_z(k_x, k_y)}{\tilde{H}(k_x, k_y)(k_x^2 + k_y^2)}e^{-ik_xx - ik_yy}dk_xdk_y. \quad (6)$$

We note that this solution requires regularization, since the function $\tilde{H}(k_x, k_y)$ has near-zero values at high spatial frequencies, leading to divergence of the solution during division, when the field-measurement noise is insignificant.

EXPERIMENTAL STUDIES

A device based on a matrix that consists of 64 flat spiral rectangular induction coils was designed to perform the experimental studies (Fig. 2). Each coil has dimensions of 19 × 19 mm. The coils are placed in four rows with a 20-mm step along the axis. Each row is shifted relative to the previous one by 5 mm along the y-axis and by 20 mm along the x-axis. Thus, while scanning along the X-axis with a 5-mm step, the measurements along the y-axis will be also carried out with a 5-mm step. An STM32 F407 microcontroller was used to control the device. Using the DAC of the microcontroller, a sinusoidal signal is applied to the coil–source through an amplifier. The signal frequency can vary from 3 to 22 kHz. The receiving coil matrix is connected through multiplexers to the ADC of the microcontroller. Since the DAC and ADC of

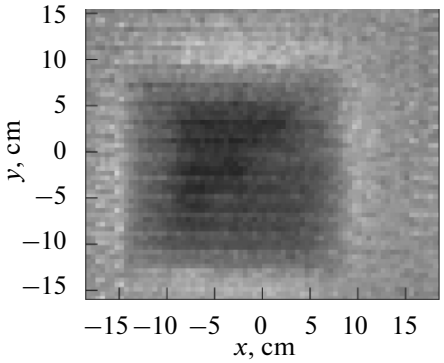

Fig. 3. The cosine quadrature of the signal from the receiving coils at 3 kHz.

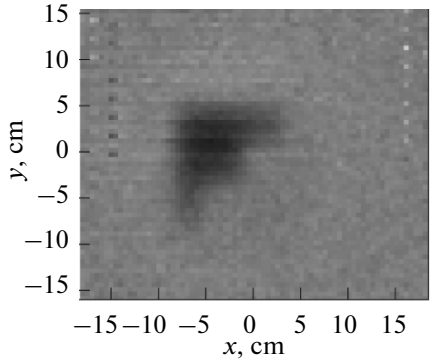

Fig. 4. The sine quadrature of the signal from the receiving coils at 3 kHz.

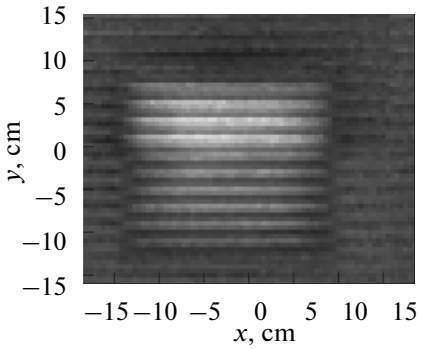

Fig. 5. The cosine quadrature of the signal from the receiving coils at 22 kHz.

the microcontroller are synchronized, this allows one to measure not only the amplitude but the phase of the signal.

In the course of the experiments several types of flat metal objects were studied, namely, a stepped brass triangle that was hidden behind aluminum foil (with a thickness of 30 μm) with a 5-mm gap; a brass plate with a narrow cut (1 mm); and an aluminum triangle with a wide cut (15 mm). All the objects were probed at a distance of 1 cm. As a result of the measurements, the quadratures of the signals were derived in the receiving coils. The measurement area was 37 × 32 cm with a 5-mm step. One scanning required approximately 30 seconds.

RESULTS AND DISCUSSION

As a result of the experiment with the stepped triangle that was concealed behind aluminum foil, the quadratures of signals at different frequencies were obtained (Figs. 3–6). One can see that the field pene-

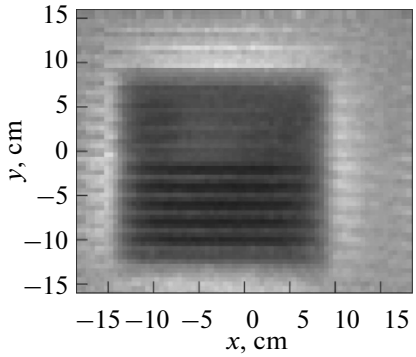

Fig. 6. The sine quadrature of the signal from the receiving coils at 22 kHz.

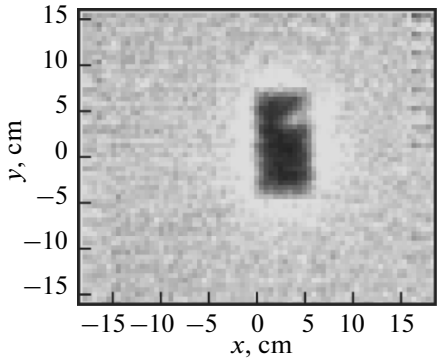

Fig. 7. The amplitude of the signal from the receiving coils for a plate with a 1-mm-thick cut.

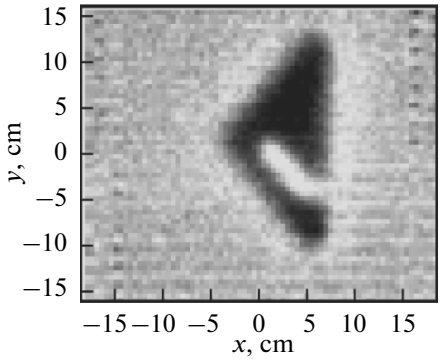

Fig. 8. The amplitude of the signal from the receiving coils for a plate with a 15-mm-thick cut.

trated through the aluminum foil at 3 kHz (the skin-layer is 1.5 mm at a frequency of 3 kHz) and the image of the concealed object was observed. At 22 kHz (the skin-layer is 0.55 mm at a frequency of 22 kHz) the field penetrated through the foil insufficiently for visualizing the concealed object; hence, only the foil was visualized.

This result allows one to state that measurements at different frequencies determine the presence of a concealed object and evaluate which of the objects is located farther or closer. The object that was distinguished in the measurements at high frequencies was located nearer to the receiving coil matrix. The object that is seen in the measurements at low frequencies was located farther from the matrix.

As a result of the experiments with the metal plates with cuts, their images, on which the cuts are clearly visualized, were obtained at 10 kHz (Figs. 7 and 8). Note that the cut width is not of great significance, since the main issue is the absence of electric contact in the cut.

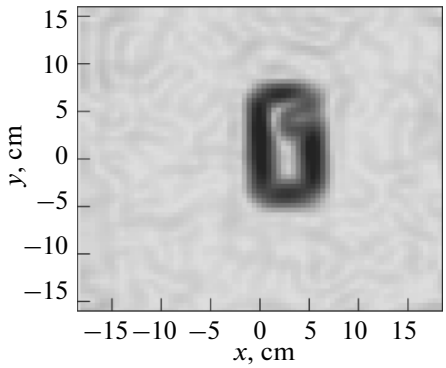

Fig. 9. The module of the induction-current vector for a plate with a 1-mm-thick cut.

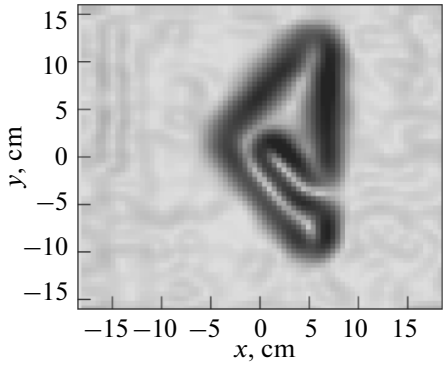

Fig. 10. The module of the induction-current vector for a plate with a 15-mm-thick cut.

Formally, the resolution of the system is evaluated by the gap value between uniform regions at which these regions are distinguishable, i.e., the resolution proved to be smaller than 1 mm, which is comparable with the resolution of the *x*-ray method. However, in our case, it is impossible to evaluate the particular thickness of the gap if the distance between the uniform regions is smaller than the distance to the measuring system (in this case, 1 cm). If the resolution over the width of the spatial spectrum of the restored image is evaluated it will show that it is approximately equal to the distance to the object.

The restoration method of induction currents from measurements of only the *z*-component of the magnetic-induction vector was applied to the results of this experiment. The current restoration results are shown in Figs. 9 and 10.

One can see that the current follows the object contour; on the whole it is in accord with the induction-current behavior.

CONCLUSIONS

A magnetic introscope that allows one to visualize electroconductive objects that are concealed behind metal barriers and to detect flaws in the form of *cuts* in metal plates was designed. A method for restoring the induction-current distribution was tested using experimental data. The resolution of the system, as evaluated via the image quality, is comparable with the distance to the object. However, it is possible to distinguish two objects at an arbitrarily close distance in the absence of an electric contact between them.

ACKNOWLEDGMENTS

This work was supported by the Russian Federation Ministry of Education and Science as part of state job no. 3.694.2014/K and Program for raising the competitive capacity of Tomsk State University.

REFERENCES

1. Shur, M.L., Novoslugina, A.P., and Smorodinskii, Ya.G., On the inverse problem of magnetostatics, *Russ. J. Nondestr. Test.*, 2013, no. 8, p. 465.
2. Pavlyuchenko, V.V. and Doroshevich, E.S., Nondestructive control of objects made of electroconductive materials in pulsed magnetic fields, *Russ. J. Nondestr. Test.,* 2010, no. 11, p. 810.
3. Garcia-Martin, J. and Gomez-Gilb, J., Comparative evaluation of coil and Hall probes in hole detection and thickness measurement on aluminum plates using eddy current testing, *Russ. J. Nondestr. Test.*, 2013, no. 8, p. 482.
4. Remezov, V.B., A Study of the electromagnetic fields that are generated by a coil emitter, *Russ. J. Nondestr. Test.*, 2013, no. 7, p. 365.
5. Korjenevsky, A., Cherepenin, V., and Sapetsky, S., Magnetic induction tomography: experimental realization, *Physiol. Meas.*, 2000, no. 21 (1), pp.89–94.
6. Babushkin, A.K., Bugaev, A.S., Vartanov, A.V., Korjenevsky, A.V., Sapetsky, S.A., Tuikin, T.S., and Cherepenin, V.A., Development of methods and instruments of magnetic induction tomography for studying human's brain and cognitive functions, *Izv. Akad. Nauk, Ser. Fiz.*, 2011, vol. 75, no. 1, pp. 144–148.
7. Korjenevsky, A.V., Magnetic induction tomography for medical applications, *Almanac of Clinical Medicine*, 2008, no. 17-1, pp. 1991–194.
8. Li Shu, Huang Songling, and Zhao Wei., Development of differential probes in pulsed eddy current testing for noise suppression, *Sensors and Actuators*, 2007, A 135, p. 675–679.
9. Sukhanov, D.Ya. and Goncharik, M.A., Determination of the shape of electroconductive object from remote measurements of disturbances of alternating magnetic field, *Izv. Vyssh. Uchebn. Zaved., Fiz.*, 2013, vol. 56, no. 8/2, pp. 41–43.
10. Yakubov, V.P., Shipilov, S.E., Sukhanov, D.Ya., and Klokov, A.V., *Radiovolnovaya tomografiya: dostizheniya i perspektivy* (Radio Wave Tomography: Achievements and Prospects), Tomsk: Izd-vo NTL, 2014.
11. Yakubov, V.P., Losev, D.V. and Mal'tsev, A.I., Wave tomography of absorbing media, *J. Commun. Technol. Electron*. 2004, vol. 49, no. 1, p. 54.
12. Sukhanov, D.Ya. and Berzina, E.S., Magnetic introscopy using a magnetic sensor matrix, *Izv. Vyssh. Uchebn. Zaved., Fiz.*, 2013, vol. 56, no. 8/2, pp. 23–26.

Translated by N. Pakhomova